Acta Crystallographica Section D
Biological Crystallography
ISSN 0907-4449

MRSAD: using anomalous dispersion from S atoms collected at Cu *Kα* wavelength in molecular-replacement structure determination

Jonathan P. Schuermann and John J. Tanner*

Departments of Chemistry and Biochemistry, University of Missouri-Columbia, Columbia, MO 65211, USA

Correspondence e-mail: tannerjj@missouri.edu

Received 6 March 2003
Accepted 16 July 2003

The use of single-wavelength anomalous dispersion (SAD) from S atoms collected in-house to overcome model bias in molecular-replacement (MR) structure determination is demonstrated. The test case considered is a $P6_522$ anti-ssDNA Fab crystal with a theoretical anomalous signal of 0.8% and a diffraction limit of 2.3 Å, from which a 360°, 39-fold redundant data set was collected. A nearly complete anomalous scatterer substructure could be quickly built from anomalous difference Fourier analysis based on phases from a full or partial MR solution. The resulting SAD phases were improved with density modification and used to calculate an unbiased electron-density map that could be used for model building. This map displayed clear and continuous density for almost the entire main chain, as well as good density for most side chains. The favorable results obtained from this realistic test case suggest that anomalous differences from S atoms should be routinely collected and used in MR structure determination.

1. Introduction

Molecular replacement (MR) is a widely used phasing method in macromolecular crystallography. Its popularity largely derives from its ease of use. All that is needed for structure determination is a single native data set collected at any convenient X-ray wavelength, the coordinates of a homologous protein structure to serve as the search model and a computer program that determines the orientation and position of the search model(s) in the asymmetric unit. In principle, accurate phases can be obtained in a matter of hours or even minutes.

In practice, however, sometimes structure determination by MR is not straightforward. One major problem is that maps calculated from MR phases inevitably retain some residue of the search model (model bias), which can complicate model building in areas of the structure where the search model and protein under consideration differ. Several methods have been developed to overcome model bias, but it still remains a significant issue in MR phasing (Read, 1997; Adams *et al.*, 1999; Terwilliger, 2001).

Here, we demonstrate the utility of incorporating single-wavelength anomalous dispersion (SAD) from S and P atoms collected using a standard Cu rotating-anode system in MR structure determination. An attractive feature of this strategy (denoted MRSAD) is that the anomalous scatterer substructure can be quickly determined from the MR solution. Moreover, since the SAD phases are virtually independent of the MR phases, MRSAD provides an experimental method to overcome the model bias inherent to MR.

Table 1
Data-collection statistics.

Values in parentheses are for the highest resolution shell of data.

Wavelength (Å)	1.5418
Space group	$P6_522$
Unit-cell parameters (Å)	a = 172.2, c = 144.9
No. of crystals	1
No. of molecules per AU	2
Diffraction resolution (Å)	100–2.3 (2.38–2.30)
No. of observations	2155020
No. of unique reflections	55099
Redundancy	39.1
Completeness (%)	97.2 (95.4)
Anomalous completeness (%)	89.5 (92.9)
Mean $I/\sigma(I)$	58.1 (7.5)
$R_{\rm merge}$	0.078 (0.625)
Resolution of phasing (Å)	20–3.5
Experimental $\langle\Delta F\rangle/\langle F\rangle$ (%)	1.1
Calculated $\langle\Delta F\rangle/\langle F\rangle$ (%)	0.8

2. Materials and methods

2.1. Crystallization and X-ray data collection

To demonstrate proof of concept, diffraction data were collected from a single crystal of a recombinant anti-ssDNA Fab, known as DNA-1, complexed with dT_5. The details of protein purification, crystallization and molecular-replacement calculations have been reported elsewhere (Prewitt *et al.*, 2000) and the structure itself (PDB code 1i8m) has been described (Tanner *et al.*, 2001). The asymmetric unit includes two Fab molecules (Fab 1 and Fab 2), one complete dT_5 (nucleotides T1–T5), a d(pTp) moiety bound to Fab 2 (nucleotide D2) and one sulfate ion. The light/heavy chains are denoted L/H in Fab 1 and A/B in Fab 2 (Tanner *et al.*, 2001). Each Fab has eight Cys and seven Met residues, giving a total of 30 protein S atoms in the asymmetric unit. The total molecular weight of the two Fabs plus dT_5 is about 100 kDa.

Crystals were grown in sitting drops over a reservoir of 0.1 *M* sodium acetate, 1.8–2.0 *M* ammonium sulfate pH 4.8–5.2 (Prewitt *et al.*, 2000). The crystals occupy space group $P6_522$, with unit-cell parameters $a = b = 172.2$, $c = 144.9$ Å and a solvent content of 63%. Following a short soak in 30% glycerol, the crystals were plunged into liquid nitrogen in preparation for cryogenic data collection.

X-ray diffraction data were recorded to 2.3 Å resolution with an R-AXIS IV detector coupled to a Rigaku RU-H3R copper rotating-anode generator equipped with Osmic MaxFlux confocal optics. A total of 360° of data was collected with an oscillation angle of 0.5° and an exposure time of 20 min per degree of oscillation. The crystal-to-detector distance was 200 mm and the detector angle was zero. The data were processed using *HKL* (Otwinowski & Minor, 1997). See Table 1 for data-collection statistics.

2.2. MR and SAD phase calculations

MR calculations were performed with *AMoRe* (Navaza & Saludjian, 1997) using an anti-lysozyme Fab search model (PDB code 1mlc; Braden *et al.*, 1994) and 10–3 Å resolution data. The same search model was used in the original structure determination of DNA-1/dT_5 (Tanner *et al.*, 2001). SAD phase calculations and refinement of the anomalous scatterer parameters were performed with *CNS* (Brünger *et al.*, 1998) using 20–3.5 Å resolution data with the maximum-likelihood amplitude target. These calculations included overall anisotropic B scaling, refinement of the S-atom positions, individual isotropic B-factor refinement and refinement of f''. The anomalous atomic occupancies were fixed at a value of one. The SAD phases were improved and extended to 2.3 Å resolution with density-modification calculations using *CNS*, which included density truncation, solvent flipping (Abrahams & Leslie, 1996) and non-crystallographic twofold averaging. Electron-density maps were viewed with *O* (Jones *et al.*, 1991).

3. Results

3.1. Data quality

The importance of using highly redundant data in S-SAD phasing has been emphasized previously (Debreczeni, Bunkoczi, Ma *et al.*, 2003; Ramagopal *et al.*, 2003). The data set used for this work resulted from a single 360° scan around a vertical rotation axis. Owing to the high symmetry of the crystal, the data were highly redundant, with an average of 39 observations per unique reflection (Table 1). Thus, the signal-to-noise ratio was very favorable, as evidenced by an average $I/\sigma(I)$ of 7.5 in the highest resolution shell. While this value might suggest the crystal diffracted significantly beyond 2.3 Å, the data were truncated at 2.3 Å resolution because of the rather high $R_{\rm merge}$ value of 0.63 in the highest resolution shell (Table 1). Visual inspection of diffraction images also revealed little data beyond 2.3 Å.

The quantity $\langle\Delta F\rangle/\langle F\rangle$ has been suggested as a criterion for evaluating the quality of sulfur anomalous data (Dauter *et al.*, 1999; Yang & Pflugrath, 2001). The resolution limit for SAD phase calculations was chosen such that the measured $\langle\Delta F\rangle/\langle F\rangle$ was approximately equal to the theoretical estimate of $\langle\Delta F\rangle/\langle F\rangle$. The measured $\langle\Delta F\rangle/\langle F\rangle$ was 1.1% for 20–3.5 Å data, which is close to the theoretical value of 0.8%. In contrast, the measured $\langle\Delta F\rangle/\langle F\rangle$ for the 3.5–3.0 Å shell of data was 2.0%, while the 3.0–2.5 Å shell had a $\langle\Delta F\rangle/\langle F\rangle$ value of 5.4%. The rapid increase in $\langle\Delta F\rangle/\langle F\rangle$ beyond 3.5 Å was likely to be a consequence of higher noise in the estimation of both F and ΔF (Dauter *et al.*, 1999). This analysis suggested that 3.5 Å was a reasonable high-resolution cutoff for SAD phasing.

3.2. Using MR to determine the anomalous scatterer substructure

The first step in SAD phasing is determination of the anomalous scatterer substructure. With an MR solution in hand, an initial S-atom substructure can easily be obtained using either of the two methods suggested previously (Micossi *et al.*, 2002). In the first method, the coordinates of S atoms are simply extracted from the MR solution to initiate SAD phasing. We suggest that this initial S-atom constellation should derive from conserved Cys and Met residues because

Table 2
Analysis of anomalous difference Fourier map peaks.

	Round 1 (FOM = 0.13)†		Round 2 (FOM = 0.16)†		Round 3 (FOM = 0.20)†		Round 4 (FOM = 0.22)†	
Rank	Height (σ)	Anomalous scatterer	Height (σ)	Anomalous scatterer	Height (σ)	Anomalous scatterer	Height (σ)	Anomalous scatterer
1	37.4	CysH140—CysH195‡	31.1	CysH140—CysH195‡	28.0	CysH140—CysH195‡	26.9	CysB140—CysB195‡
2	36.5	CysL23—CysL88‡	29.9	CysL23—CysL88‡	26.6	CysB140—CysB195‡	26.2	CysL134—CysL194‡
3	35.2	CysH22—CysH92‡	29.6	CysL134—CysL194‡	26.3	CysL134—CysL194‡	26.1	CysH140—CysH195‡
4	35.0	CysL134—CysL194‡	27.8	CysB140—CysB195‡	26.0	CysL23—CysL88‡	24.5	CysH22—CysH92‡
5	4.8	CysB140—CysB195	27.4	CysH22—CysH92‡	24.9	CysH22—CysH92‡	24.1	CysL23—CysL88‡
6	4.1	CysA23—CysA88	24.2	CysA134—CysA194‡	23.8	CysA134—CysA194‡	23.7	CysA134—CysA194‡
7	4.0	MetA175	23.8	CysA23—CysA88‡	21.8	CysA23—CysA88‡	21.6	MetH20‡
8	4.0	CysA134—CysA194	19.9	MetA175‡	21.2	MetH20‡	20.0	MetH80‡
9	3.6	CysB22—CysB92	4.7	MetH80	20.1	CysB22—CysB92‡	19.4	CysA23—CysA88‡
10	3.6	MetB20	4.6	MetB20	20.0	MetH80‡	19.3	MetB20‡
11	3.6		4.2		19.5	MetB20‡	18.9	MetB80‡
12	3.3	MetH100C	4.1	CysB22—CysB92	19.2	MetA175‡	18.7	CysB22—CysB92‡
13	3.3	MetB100C	3.9	MetH20	18.1	MetB80‡	17.0	MetB100C‡
14	3.2		3.8	MetB80	17.1	MetB34‡	17.0	MetA4‡
15	3.2		3.6	MetB34	16.5	MetH100C‡	16.8	MetA175‡
16	3.2	MetB80	3.6	MetH100C	14.6	MetH135‡	16.5	MetL175‡
17	3.2	MetH80	3.5	MetH135	4.8	MetB100C	16.5	MetB135‡
18	3.2		3.5		4.2	MetB135	16.4	MetB34‡
19	3.1		3.4		4.2		15.9	MetH100C‡
20	3.1		3.3		4.1	SO_4	13.5	MetH135‡
21	3.1		3.2		3.8	T4 P	4.3	
22	3.1		3.2		3.6	MetA4	4.2	T4 P
23	3.1		3.2		3.6	MetL175	4.1	SO_4
24	3.0		3.1		3.6		3.8	MetH34

† FOM is the overall figure of merit to 3.5 Å resolution of the SAD phases used to generate the anomalous difference Fourier map. ‡ These atoms were included in the SAD phase calculation.

the positions of the these S atoms are most likely to be correctly determined by MR. For example, in the Fab case the S atoms of the conserved disulfide bonds serve as a good choice for the initial anomalous scatterer substructure. In the second method, the initial S-atom coordinates are determined from the strong peaks of an anomalous difference Fourier (ADF) map calculated from the observed anomalous differences and the MR phases ($\Delta F_{\rm obs}$, $\varphi_{\rm MR} - 90^\circ$).

Once an initial constellation of S atoms has been chosen, the usual SAD phasing steps are followed. The anomalous scatterer parameters are refined, SAD phases are calculated and an ADF map is created. New sites are identified from strong peaks in the ADF map and these new sites are incorporated into the anomalous scatterer substructure. This process is iterated until the substructure is complete and finally the phase ambiguity is resolved using solvent flattening (Wang, 1985). Note that the enantiomorph ambiguity (Smith *et al.*, 2001) is not an issue in MRSAD.

As a demonstration of the first method of obtaining the S-atom substructure from MR, the eight Cys S atoms of Fab 1 from the correct MR solution were used to initiate MRSAD, which represented only 27% of the total protein S-atom substructure in the asymmetric unit. Following refinement of the anomalous scatterer parameters and SAD phase calculation, an ADF map was computed. As expected, the top four peaks of the ADF map corresponded to the four disulfide bonds used in the SAD phase calculation (Table 2, round 1). More importantly, peaks 5–10 corresponded to protein S atoms not included in the phase calculation. In fact, 14 of the 22 S atoms omitted from the phase calculation appeared in the ADF map at levels greater than 3σ (Table 2, round 1). Although none of the S atoms of Fab 2 were input to SAD phasing, 12 of the 15 S atoms of Fab 2 appeared in the ADF map at levels greater than 3σ, including all eight S atoms of the Fab 2 disulfide bonds (Table 2, round 1). The disulfide bonds, however, appeared as single peaks in the ADF map owing to the limited resolution of the analysis. A nearly complete anomalous substructure was then built in four subsequent rounds of iterative ADF map analysis and consisted of 29 of the 30 protein S atoms, one sulfate ion and one of the DNA P atoms (Table 2, rounds 2–4).

Note that the ADF map analysis provided an independent verification of the MR solution, as indicated by the excellent correspondence between the strong peaks of the ADF maps and the S-atom positions of the MR solution that were excluded from SAD phase calculations. This aspect of MRSAD could be useful in difficult MR cases.

To demonstrate the second method of obtaining the S-atom substructure, phases were calculated from the MR model following rigid-body, simulated-annealing and individual *B*-factor refinements in *CNS* to $R = 0.29$ and $R_{\rm free} = 0.34$. These phases were then used to calculate an ADF map ($\Delta F_{\rm obs}$, $\varphi_{\rm MR} - 90^\circ$). All but two of the top 30 peaks of the map corresponded to S or P atoms of the known structure (PDB code 1i8m) and all the S atoms of the protein appeared above the 5σ level (Table 3). All four P atoms of the dT_5 ligand appeared within the top 35 peaks at levels of 4.7–7.0σ, confirming the location of this ligand. Thus, a nearly complete anomalous substructure could be built from a single ADF map, which suggested that this method of obtaining the

Table 3
Peaks of anomalous difference Fourier map based on MR phases (ΔF, $\varphi_{MR} - 90^\circ$).

Peak	Height (σ)	Anomalous scatterer
1	12.0	CysB140—CysB195
2	11.1	MetH80
3	10.7	CysL23—CysL88
4	10.6	CysL134—CysL194
5	10.6	CysB22—CysB92
6	10.4	CysH22—CysH92
7	10.3	MetB80
8	10.0	CysA23—CysA88
9	9.9	CysA134—CysA194
10	9.9	CysH22—CysH92
11	9.4	MetB20
12	9.3	MetL4
13	9.2	MetH20
14	9.0	MetH34
15	8.8	MetB100C
16	8.5	CysH100C
17	8.5	MetB34
18	8.4	CysH140—CysH195
19	7.7	MetA175
20	7.4	MetH135
21	7.1	MetB135
22	7.0	CysA134—CysA194
23	7.0	T4 P
24	6.9	Solvent
25	6.4	MetA4
26	6.3	SO_4
27	6.1	CysL23—CysL88
28	5.8	T5 P
29	5.4	Solvent
30	5.3	MetL175
31	5.3	MetL175
32	5.1	T3 P
33	4.9	
34	4.7	
35	4.7	T2 P
36	4.7	Solvent
37	4.7	CysA23—CysA88
38	4.6	Solvent

anomalous substructure was superior to the approach of extracting S atoms from the MR solution. In fact, even phases calculated from a partial MR solution were good enough to identify the S-atom substructure. For example, when Fab 2 of the MR solution was omitted from the phase calculation, the ADF map clearly showed the positions of all the protein S atoms, including those of Fab 2 (Fig. 1).

3.3. Unbiased maps for model building

SAD phases (φ_{SAD}) were calculated to 3.5 Å resolution using a 39-atom anomalous substructure derived from the (ΔF_{obs}, $\varphi_{MR} - 90^\circ$) ADF map (see Table 3). The figure of merit and Cullis *R* factor were 0.24 and 0.71, respectively. The phases were improved and extended to 2.3 Å resolution with density modification. The density-modified SAD phases ($\varphi_{SAD\text{-}DM}$) had a phase difference of 67° relative to those calculated from the known structure (1i8m), while the figure-of-merit-weighted map correlation coefficient was 0.63. These statistical indicators are similar to those quoted in other successful SAD phasing studies (Yang & Pflugrath, 2001; Dauter *et al.*, 2002). The SAD map displayed clear and continuous density for almost the entire main chain and it had good density indicating the positions of most side chains (Fig. 2). Thus, MRSAD produced a bias-free map that was of sufficient quality to guide detailed model building.

Figure 1
Anomalous difference Fourier map calculated from a partial MR solution (ΔF_{obs}, $\varphi_{MR\text{-}PART} - 90^\circ$) covering Fab 2 of the known structure (1i8m). The partial MR solution consisted of Fab 1 of the full MR solution, while Fab 2 was omitted. The 11 strong density features represent the entire S-atom substructure of one Fab: four disulfide bonds and seven Met residues. The map was contoured at 3.5σ. This figure was created with *MOLSCRIPT* (Kraulis, 1991), *BOBSCRIPT* (Esnouf, 1997) and *Raster3D* (Merritt & Murphy, 1994).

4. Discussion

This paper demonstrates a simple approach for overcoming model bias in MR structure determination using S-SAD data collected using Cu $K\alpha$ radiation. An attractive aspect of MRSAD is that the initial S-atom substructure used for SAD

phasing is quickly obtained from the MR solution, either by extracting S-atom coordinates from the MR model or, preferably, by ADF map analysis based on MR phases. These simple methods contrast with more sophisticated and potentially laborious approaches based on Patterson maps and dual-space methods (Xu *et al.*, 2002; Usón *et al.*, 2003). The method of using the MR solution to bootstrap SAD phasing was essential for the Fab test case presented here because attempts to determine the S-atom substructure using *CNS*, *SOLVE* (Terwilliger & Berendzen, 1999) and *SnB* (Weeks & Miller, 1999) failed in our hands. These programs failed, in part, because the S atoms of disulfide bonds cannot be resolved at 3.5 Å resolution. When all 16 disulfide S atoms were given to the *CNS* anomalous difference Patterson solving program as pre-existing sites, for example, the locations of ten of the 14 Met S atoms could be found. Similar difficulties have been reported recently (Usón *et al.*, 2003).

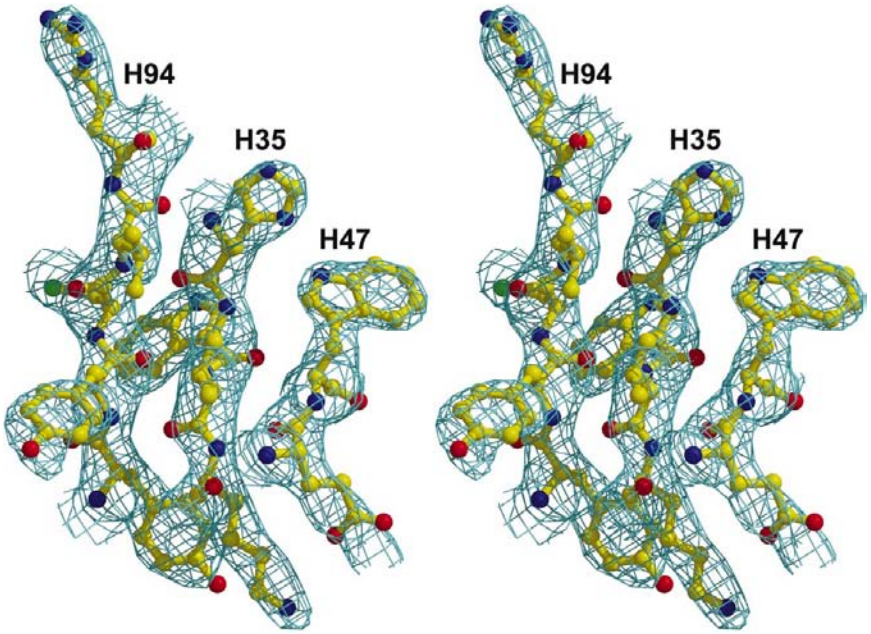

Figure 2
A figure-of-merit-weighted, density-modified SAD map (FOM*F_{obs}, $\varphi_{SAD\text{-}DM}$) covering the known structure (1i8m). SAD phases were calculated to 3.5 Å resolution from an anomalous substructure of 39 atoms (see Table 3) and then improved and extended to 2.3 Å resolution with density truncation, solvent flipping and NCS averaging. The map is contoured at 1σ.

The crystal used in this study diffracted to 2.3 Å resolution and the theoretical anomalous signal was only 0.8%. Thus, we applied the MRSAD strategy to a realistic test case in order to demonstrate the limits of the method. Despite the weak anomalous signal of the system studied, the MRSAD approach was shown to be useful for confirming the MR solution, locating bound ligands containing S and P atoms and verifying the main-chain trace. More importantly, the MRSAD method led to a high-quality unbiased electron-density map for model building. Thus, one could imagine using the MR solution solely for the purpose of bootstrapping sulfur-SAD phasing using the MRSAD strategy and then performing all model building with the unbiased SAD map rather than the potentially biased MR maps.

The results presented here support the assertion that anomalous differences from S atoms should be routinely collected and used in macromolecular structure determination when using a standard Cu rotating-anode system (Lehmann & Pebay-Peyroula, 1992; Dauter *et al.*, 1999, 2002; Yang & Pflugrath, 2001; Lemke *et al.*, 2002; Debreczeni, Bunkoczi, Girmann *et al.*, 2003). We would extend this assertion to include cases in which MR is to be used, particularly if one anticipates problems in MR phasing. The extra human effort expended in data collection is negligible: one simply allows the data collection to continue for longer than usual. The extra computational effort is also minimal because the S-atom substructure is quickly determined from the MR search model.

We wish to thank Mitchell D. Miller for insightful discussions and critical reading of the manuscript.

References

Abrahams, J. P. & Leslie, A. G. W. (1996). *Acta Cryst.* D**52**, 30–42.
Adams, P. D., Pannu, N. S., Read, R. J. & Brunger, A. T. (1999). *Acta Cryst.* D**55**, 181–190.
Braden, B. C., Souchon, H., Eisele, J. L., Bentley, G. A., Bhat, T. N., Navaza, J. & Poljak, R. J. (1994). *J. Mol. Biol.* **243**, 767–781.
Brünger, A. T., Adams, P. D., Clore, G. M., DeLano, W. L., Gros, P., Grosse-Kunstleve, R. W., Jiang, J. S., Kuszewski, J., Nilges, M., Pannu, N. S., Read, R. J., Rice, L. M., Simonson, T. & Warren, G. L. (1998). *Acta Cryst.* D**54**, 905–921.
Dauter, Z., Dauter, M., de La Fortelle, E., Bricogne, G. & Sheldrick, G. M. (1999). *J Mol. Biol.* **289**, 83–92.
Dauter, Z., Dauter, M. & Dodson, E. (2002). *Acta Cryst.* D**58**, 494–506.
Debreczeni, J. E., Bunkoczi, G., Girmann, B. & Sheldrick, G. M. (2003). *Acta Cryst.* D**59**, 393–395.
Debreczeni, J. E., Bunkoczi, G., Ma, Q., Blaser, H. & Sheldrick, G. M. (2003). *Acta Cryst.* D**59**, 688–696.
Esnouf, R. M. (1997). *J. Mol. Graph.* **15**, 132–134.
Jones, T. A., Zou, J.-Y., Cowan, S. W. & Kjeldgaard, M. (1991). *Acta Cryst.* A**47**, 110–119.
Kraulis, P. J. (1991). *J. Appl. Cryst.* **24**, 946–950.
Lehmann, M. S. & Pebay-Peyroula, E. (1992). *Acta Cryst.* B**48**, 115–116.
Lemke, C. T., Smith, G. D. & Howell, P. L. (2002). *Acta Cryst.* D**58**, 2096–2101.
Merritt, E. A. & Murphy, M. E. P. (1994). *Acta Cryst.* D**50**, 869–873.
Micossi, E., Hunter, W. N. & Leonard, G. A. (2002). *Acta Cryst.* D**58**, 21–28.
Navaza, J. & Saludjian, P. (1997). *Methods Enzymol.* **276**, 581–594.
Otwinowski, Z. & Minor, W. (1997). *Methods Enzymol.* **276**, 307–326.
Prewitt, S. P., Komissarov, A. A., Deutscher, S. L. & Tanner, J. J. (2000). *Acta Cryst.* D**56**, 1007–1011.
Ramagopal, U. A., Dauter, M. & Dauter, Z. (2003). *Acta Cryst.* D**59**, 1020–1027.

Read, R. J. (1997). *Methods Enzymol.* **277**, 110–128.
Smith, J. L., Hendrickson, W. A., Terwilliger, T. C. & Berendzen, J. (2001). *International Tables for Crystallography*, Vol. F, edited by M. G. Rossmann & E. Arnold, pp. 299–309. Dordrecht: Kluwer Academic Publishers.
Tanner, J. J., Komissarov, A. A. & Deutscher, S. L. (2001). *J. Mol. Biol.* **314**, 807–822.
Terwilliger, T. C. (2001). *Acta Cryst.* D**57**, 1763–1775.
Terwilliger, T. C. & Berendzen, J. (1999). *Acta Cryst.* D**55**, 849–861.
Usón, I., Schmidt, B., Von Bulow, R., Grimme, S., Von Figura, K., Dauter, M., Rajashankar, K. R., Dauter, Z. & Sheldrick, G. M. (2003). *Acta Cryst.* D**59**, 57–66.
Wang, B.-C. (1985). *Methods. Enzymol.* **115**, 90–112.
Weeks, C. M. & Miller, R. (1999). *J. Appl. Cryst.* **32**, 120–124.
Xu, H., Hauptman, H. A. & Weeks, C. M. (2002). *Acta Cryst.* D**58**, 90–96.
Yang, C. & Pflugrath, J. W. (2001). *Acta Cryst.* D**57**, 1480–1490.